

Determination of Mechano-sorptive Coefficients in *Eucalyptus nitens* Wood under Isothermal Conditions

Carlos Salinas,^a Cristian Chávez,^{b,*} Francisco Cárdenas,^a José Torres,^c and Rubén Ananías^c

New experimental data is presented for the mechano-sorptive coefficient of *Eucalyptus nitens* wood analyzed in the longitudinal direction through the principle of total deformation superposition. The procedure was based on the determination of the partial strain components: elastic strain, free shrinkage strain, and mechano-sorptive strain. The methodology included the design of cantilever flexion tests of a wooden beam in an air-conditioned environment with variable relative humidity. These conditions made it possible to estimate each of the deformation components separately and then to determine the mechano-sorptive coefficient using the rheological stress-strain model. Deformations and displacements were evaluated with extensometers and displacement sensors, respectively, in conditions of 0 to 30% of the breaking load applied perpendicularly to beams oriented in the longitudinal direction. The cross-section was positioned according to the relation between the action line of the load applied and the growth rings orientation. The variation of moisture content was considered, decreasing from 22 to 12%. The results exposed a direct proportionality between the intensity of the applied load and the mechano-sorptive strains. The values determined for mechano-sorptive coefficients were 0.1224 and 0.1746 GPa⁻¹ for loads applied to radial and tangential directions, respectively.

DOI: 10.15376/biores.17.1.1047-1061

Keywords: Drying stresses; Stress-strain; Elasticity; Free shrinkage; Moisture content

Contact information: a: Department of Mechanical Engineering, Research Laboratory on Wood Drying & Heat Treatments, University of Bío-Bío, Concepción, Chile; b: Department of Mechanical Engineering, University of La Serena, La Serena, Chile; c: Department of Wood Engineering, Research Laboratory on Wood Drying & Heat Treatments, University of Bío-Bío, Concepción Chile;

* Corresponding author: cchavez@userena.cl

INTRODUCTION

Eucalyptus nitens is a fast-growing species used primarily in the pulp industry, while a part of its production is transformed into solid wood products (Infor 2018). Recently, the potential of the species for structural purposes and applications related to wood construction have been shown (Derikvand *et al.* 2017). However, the quality of *Eucalyptus nitens* products is conditioned mainly by the typical problems of solid wood during the drying process. In particular, the heterogeneous structure and density frequently lead to superficial and internal checking (Rebolledo *et al.* 2013), collapse (Ananías *et al.* 2014), as well as moisture gradients that induce mechanical stresses leading to deformations (Sepúlveda *et al.* 2016). On the other hand, given the hygroscopic nature of the wood, being exposed in service to loads in varying conditions of humidity of the environment, viscoelastic and mechano-sorptive creep are expected to occur (Armstrong and Christensen 1961; Martensson 1994; Kaboorani *et al.* 2013; Huang 2016).

When the wood is subjected to loads, it presents a particular mechanical behavior that interacts with the environment where it is located. This material exchanges energy and mass with its environment by modifying its properties and consequently develops mechanical responses of different nature (Salinas *et al.* 2015; Sepúlveda *et al.* 2016; Chávez *et al.* 2021). These can be described using the follows terms: (i) instantaneous elastic relationship between stress and strain through the module of elasticity (MOE); (ii) plastic when the stresses exceed the elastic limit; (iii) free induced by moisture content variation; (iv) mechano-sorptive related to moisture variations below the fiber saturation point (FSP); and (v) viscoelastic related to sustained loads over time (Pang 2000).

The literature presents several works related to the determination of the mechanical response of wood. In particular, a procedure consists of measuring the deformations of the wood due to the variation of humidity and temperature during heat treatment processes (Ranta-Maunus 1975; Pang 2000; Sepúlveda *et al.* 2016). Mathematical modeling has been applied to simulate the qualitative behavior of the mechanical response during drying processes (Ormarsson *et al.* 2003; Salinas *et al.* 2015; Huc *et al.* 2018). In each of these works, the authors separately evaluated the deformation components and consequently determined the mechanical response related to each contribution. In this context, the determination of each of the deformations makes it possible to isolate the response due to mechano-sorption and estimate its proportionality coefficient described in the work of Pérez *et al.* (2018). However, due to the high anatomical complexity of the wood, the calculation and determination of each component is an open topic in the literature.

Structural wood put into service and subjected to loads exhibits deformations in the radial, tangential, and longitudinal directions. In particular, the work of Pérez *et al.* (2018) presents the determination of the mechano-sorptive coefficients in the radial and tangential directions. However, the deformation due to mechano-sorption in the longitudinal direction is significant, and its study would allow greater control over the behavior of wood subjected to loads (Ranta-Maunus 1975). The longitudinal deformation by mechano-sorption in wood is explained by the coupling of micropores formation, micro-fibrils relaxation, and rearrangement of sorption sites in the cell wall of the fibers (Peng *et al.* 2017). Besides, this deformation can amount to 20 times the free shrinkage (Grossman 1976). It can be intensified when the temperature exceeds 60 °C (Hsieh and Chang 2018), when the ambient humidity increases (Florisson *et al.* 2019), or with the increase in the number of cycles of changes in humidity (Mussynski *et al.* 2006; Hering and Niemz 2012). About the behavior of *Eucalyptus nitens*, it has been shown that deformation by mechano-sorption in the transverse direction increases with the magnitude of the load and with the humidity cycles, and its development is conditioned by the anatomical orientation (Pérez *et al.* 2018).

In this context, this article presents new experimental data of the mechano-sorptive behavior of *Eucalyptus nitens*. The coefficient of proportionality between the mechano-sorptive strain and the moisture gradient will be determined when the action line of applied load was oriented at radial and tangential directions, for a beam in longitudinal bending.

EXPERIMENTAL

Material and Experimental Procedure

The materials used in this study came from 256 boards of 15-year-old *Eucalyptus nitens* wood of 2770 mm × 152 mm × 25 mm, from plantations of Los Angeles, in the

region of Bío Bío, Chile, provided by the CMPC-Maderas Spa company. The wood was heat-treated in a convective dryer to the moisture content of 10% according to the drying program described in Table 1. In particular, to evaluate effects on deformations, deflections, breakage, and variation of moisture content MC, 40 samples of $4 \times 25 \times 110 \text{ mm}^3$ were made, obtained from 10 randomly selected boards. Figure 1 shows the average of the microdensities of the tested samples. This figure shows that the microdensity (380 kg/m^3) between the earlywood rings was low and that the magnitude (530 kg/m^3) of the average microdensity of the ring was mainly conditioned by the high value (570 kg/m^3) of the microdensity of the latewood ring. The samples were obtained with a rectangular section in a transverse plane oriented in the radial-tangential (R-T) directions and the length in the longitudinal direction (L). Before the evaluations, the samples were conditioned to 22% MC in the equipment of water vapor analog control bath (Selecta, Precisterm 6000138, Barcelona, Spain) with a precision of $\pm 1 \text{ }^\circ\text{C}$, in which the MC was measured with a resistive digital moisture meter (Rdm3, Delmhorst, USA).

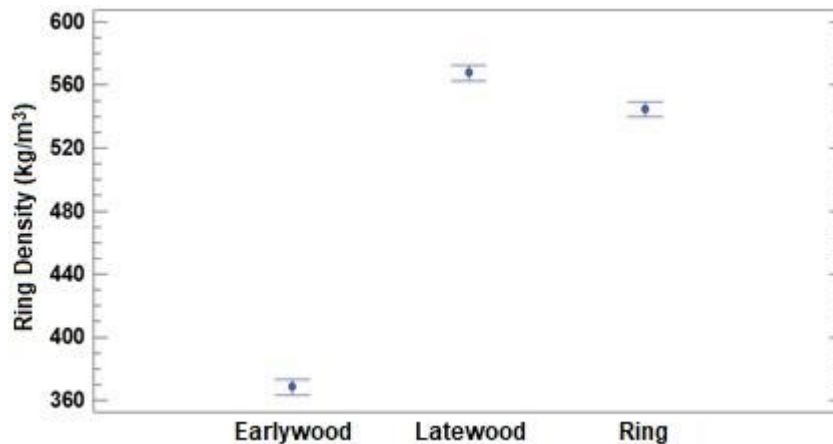


Fig. 1. Average micro density between growth rings

Table 1. Drying Program

| Tdb ($^\circ\text{C}$) | Twb ($^\circ\text{C}$) | V _{air} (%) | RH (%) | EMC (%) | Time (h) |
|--------------------------|--------------------------|----------------------|-------------------|---------|----------|
| 35 | 34 | 25 | 93 | 22 | 20 |
| 36 | 34 | 25 | 87 | 18 | 50 |
| 40 | 37 | 27 | 82 | 16 | 60 |
| 50 | 40 | 30 | 73 | 13 | 60 |
| 56 | 42 | 30 | 62 | 10 | 60 |
| 100 | 100 | 35 | collapse recovery | | 8 |
| 70 | 60 | 60 | | | 76 |

The study contemplated the performance of two tests for loads applied in the radial and tangential directions with two repetitions of which average values were obtained. The samples were arranged as a cantilever beam and exposed to four load levels, at 0, 10, 20, and 30% of the breaking load in an environment conditioned at a temperature of $20 \text{ }^\circ\text{C}$ and relative humidity (RH) of 68%. These conditions produced a continuous decreasing variation of MC from approximately 22 to 12%. Figure 2 illustrates the device implemented to apply loads with different magnitudes simultaneously, which allows recording the deformations and deflections presented by each piece of wood. In each cantilever sample, strain gauge and linear variable displacement transducer (LVDT)

sensors were installed, through which the continuous variation of the strains and vertical displacements were monitored by a data-logger (Tokyo Sokki, TDS-540, Tokyo, Japan). The tests were carried out in a time of 720 minutes.



Fig. 2. Assembly of the test: four beams installed in cantilever exposed to different conditions of concentrated load (no load, 10%, 20%, and 30%), with continuous monitoring of stresses and vertical displacement

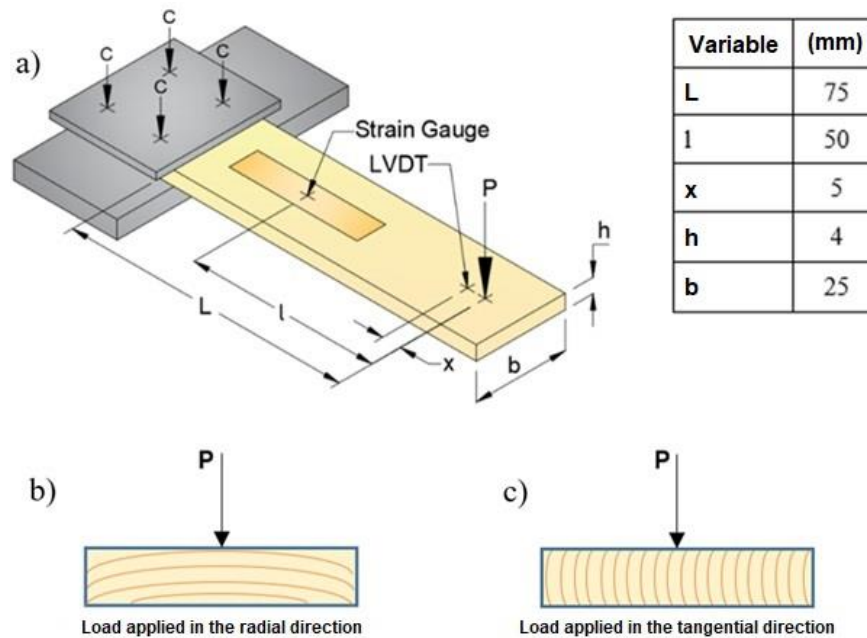


Fig. 3. a) scheme of cantilever sample $4 \times 25 \times 110 \text{ mm}^3$: concentrated load (P), strain gauges positioning, vertical displacement evaluation with LVDT; illustration of the applied load according to the direction of the wood rings: b) radial; c) tangential

Figure 3 illustrates the arrangement of the extensometers used to measure the deformations in each wood sample. Furthermore, this figure shows two cross-sectional drawings of the wood, which indicated the direction of the applied load concerning the orientation of the growth rings. The extensometers used are strain gauges TML type, of PFLW series and glued with cyanoacrylate (CN-E) on the top surface of the sample at 25 mm from the cantilever. The precision of the strain gauge was $\pm 0.1 \mu\text{m}/\text{mm}$. The gauges were oriented to measure deformations in the longitudinal direction of the wood by one gauge connected in each sample for the 4 load levels. Deflections were measured 5 mm from load application point and 15 mm from the free end through LVDT model FDP-50^a, TML brand. Deformation and deflection data were recorded by the data-logger TDS 540, TML, at intervals of one minute. The precision of the data logger is $\pm 0.1 \times 10^{-6}$.

Data Reduction Procedure

The data processing was carried out to determine the mechano-sorptive coefficient in the longitudinal direction of the wood. In this case, the breaking load was determined through the constant increment of the load applied at a rate of 1 N/s until the test piece rupture was obtained. On the other hand, the variation of MC was calculated using the gravimetric method.

Based on the principle of strain superposition, according to the independent activation model (Navi and Heger 2005), the total deformation (ε) of the wood is given by the following equation,

$$\varepsilon = \varepsilon_e + \varepsilon_v + \varepsilon_{ms} + \varepsilon_M + \varepsilon_p \quad (1)$$

where ε_e is the elastic deformation, ε_v is the viscoelastic deformation, ε_{ms} is the deformation by mechano-sorptive stress, ε_M is the free shrinkage, and ε_p is the deformation by plastic. However, for mechanical stresses that do not exceed the elastic limit and in which the test time is less than 24 h, viscoelastic and plastic deformations can be omitted (Pérez *et al.* 2016). According to this hypothesis, the deformation of the wood can be expressed in a simplified way by the following equation:

$$\varepsilon = \varepsilon_e + \varepsilon_{ms} + \varepsilon_M \quad (2)$$

In this case, if the component related to the elastic deformation is equivalent to the instantaneous strain in the initial time t_0 that $\varepsilon_e = \varepsilon_e(t=t_0)$, and that the free shrinkage is due to the MC variation (ΔMC), can be obtained from Eq. 2 strain by stresses. That is, $\varepsilon_{ms} = \varepsilon - \varepsilon_e - \varepsilon_M$, which is schematized in Fig. 4.

Finally, the mechano-sorptive coefficient (ms) was determined based on the mechanical sorption strain model for a constant stress state, Ranta-Maunus (1993), according to the following equation:

$$\frac{\partial \varepsilon_{ms}}{\partial t} = ms \cdot \sigma \cdot \frac{\partial \text{MC}}{\partial t} \rightarrow ms = \frac{1}{\sigma} \frac{\partial \varepsilon_{ms}}{\partial \text{MC}} \quad (3)$$

The stress σ and additionally the modulus of elasticity E were determined based on the displacements δ_x measured by LVDT. Then, assuming that the elastic behavior is linear and homogeneous, E is determined according to Eq. 4 and 6, respectively.

$$\sigma_e = E \varepsilon_e \quad (4)$$

$$\sigma_e = \frac{P \cdot l \cdot h}{2I} \tag{5}$$

$$E = \frac{P(L-x)^2}{2\delta_x I} \cdot \left[L - \frac{(L-x)}{3} \right] \tag{6}$$

where P is the applied load; L is the distance between the fixed end and the point of application of the load; h is the thickness of the beam; I is the moment of inertia; x is the distance between the application of the load and positioning of the LVDT; and δ_x is the vertical displacement (see Fig. 2).

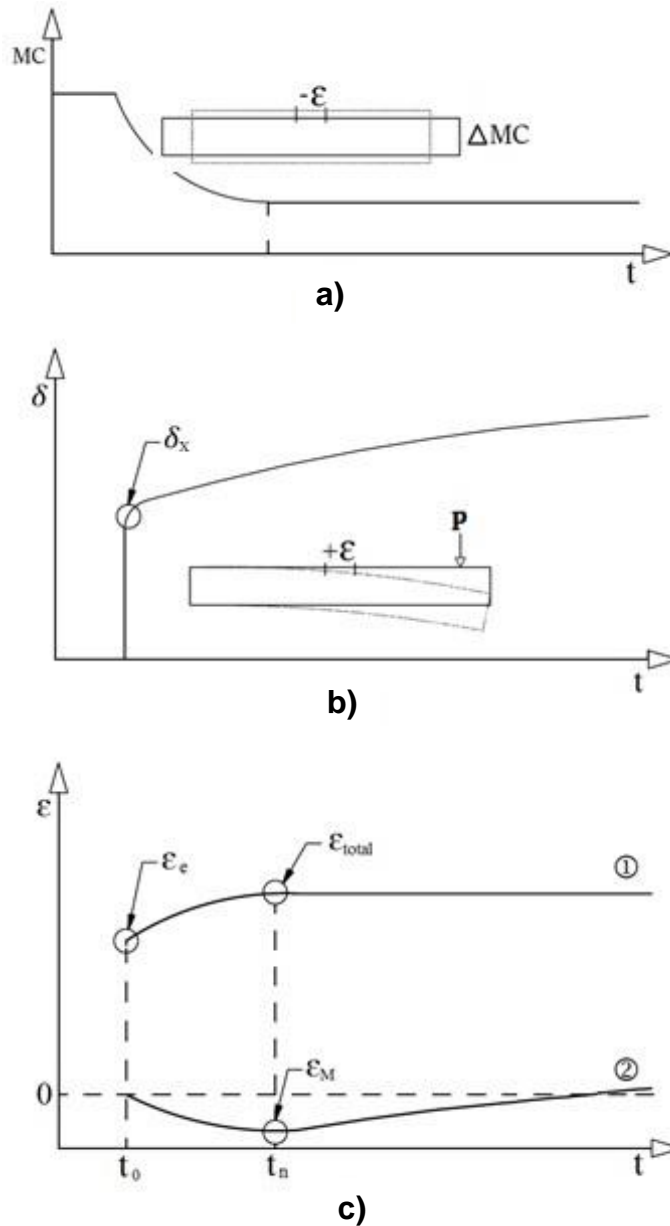


Fig. 4. Desorption strain component scheme: a) MC variation under FSP→ free shrinkage, b) deflection → surface traction, c) deformation of sample loaded (1) and not loaded (2)

RESULTS AND DISCUSSION

The results were obtained in a decreasing range of moisture content variation for values lower than fiber saturation point (FSP). Figure 5 depicts the evolution of the moisture content with the variation of time.

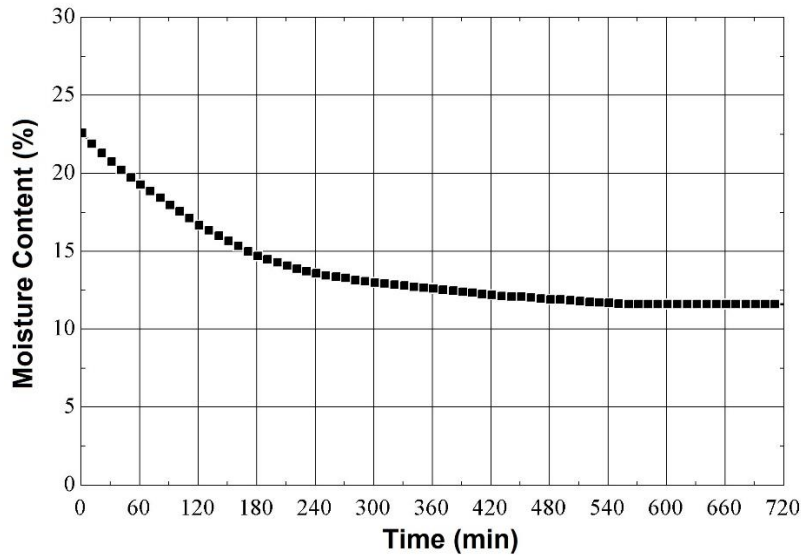


Fig. 5. Moisture content change with the time variation

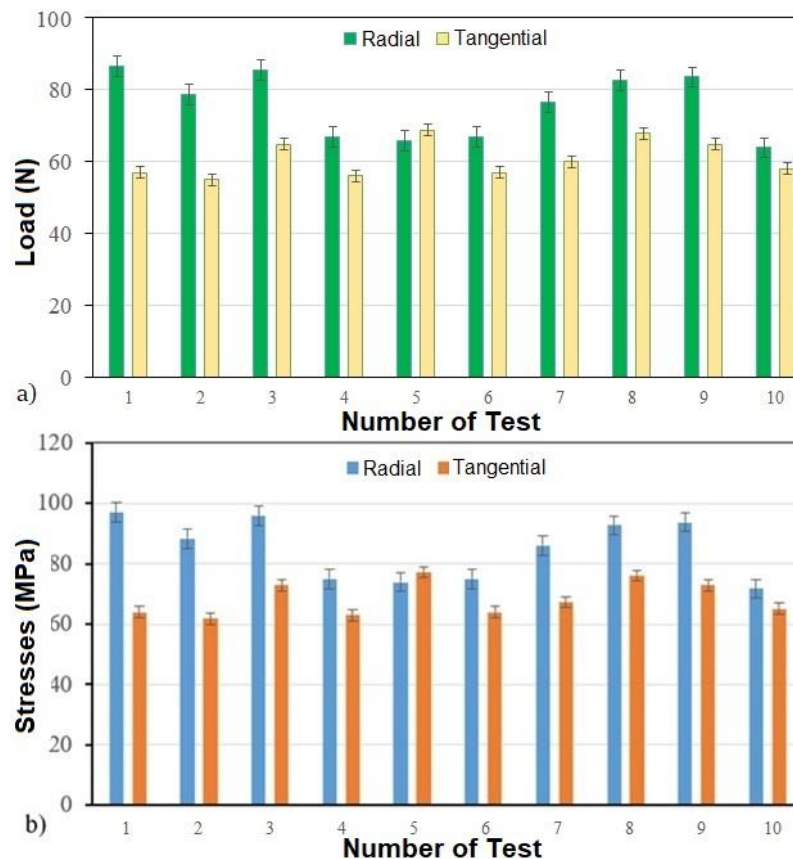


Fig. 6. Breaking loads (a) and stresses (b) in the radial and tangential directions

In Fig. 6, the MC interval starts at MC = 22% and the equilibrium moisture content corresponds to MC = 12%, which was observed up to 721 min into the process. Measuring the parameters within this moisture content range allowed evaluating the mechano-sorptive behavior. Figure 6a shows the results obtained in the tests of cantilever flexion failure (breakage) at MC = 22% with loads applied in the radial and tangential directions. Figure 6b illustrates the stresses calculated from the load data and using Eq. 5. On average, the breaking load was equal to 68 N with its stress of 76.7 MPa and the resistance in the radial direction was 24% higher than its equivalent in the tangential direction. This behavior was the result of the effect of the mechanical properties of the wood conditioned by the direction of the growth rings. In this way, the wood presented greater resistance in the load condition in the radial direction as is also indicated by McKimm (1985).

The MOE was assumed as constant according to each direction and for each of the applied loads. Figure 7 shows the change of average results of MOE with the percentage of load and the orientation of the concentrated load. The MOE can be calculated using the Eq. 6 or can be determined from the slope of the curve stress v/s strain (σ v/s ϵ). In this work, the calculation procedure was carried out using Eq. 6, and its average results were those shown in Fig. 7. In this figure, relative uniformity of values was observed. In this regard, the data were analyzed using the ANOVA procedure, which did not show significant differences for a 95% confidence interval and with average values equal to 9.4 and 8.7 GPa for the loads applied in the radial and tangential directions, respectively.

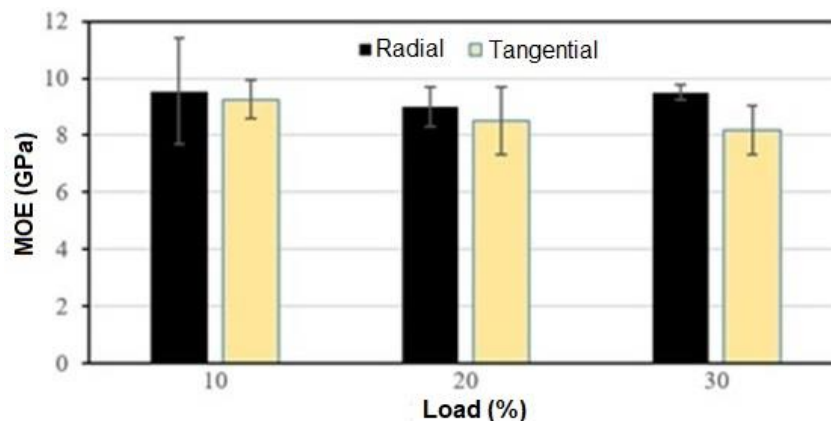


Fig. 7. MOE averages according to direction (radial and tangential) and intensity of the load (10, 20 and 30% of the breaking load)

Figure 8 displays the evolution of the deflections and total deformation. In particular, Figs. 8a and 8b compare the deflection measured for constant loads applied simultaneously on four specimens assumed to be identical. The applied loads correspond to 0, 10, 20, and 30% of the breaking limit, respectively. According to these figures, the deflection increased with the decrease of MC (desorption process). On the other hand, the tests on the samples with the load applied in a tangential direction showed higher deflections for all the curves with the applied load. This behavior was the result of the orientation of the growth rings in the cross-section of the specimen (see Fig. 3) and can be explained by the longitudinal arrangement of wood cells present in the radial direction.

Figures 8c and 8d show the total strains measured for the applied load in radial and tangential directions, respectively. In both figures, it was observed that, for the case of an applied load equal to zero, the total strain was minimal and depended mainly on the free

shrinkage strain characterized by a curvature with a positive concavity in the initial stage of the process. The strain values increased with increasing applied load. This behavior was because the total strain now depended on the components of free shrinkage, elastic, and mechano-sorptive strains. From the results of Fig. 8 and applying the procedure described in Eqs. 2 to 5, the mechano-sorptive strain can be calculated ($\varepsilon_{ms} = \varepsilon - \varepsilon_e - \varepsilon_M$). These results are presented in Table 2 and Fig. 9.

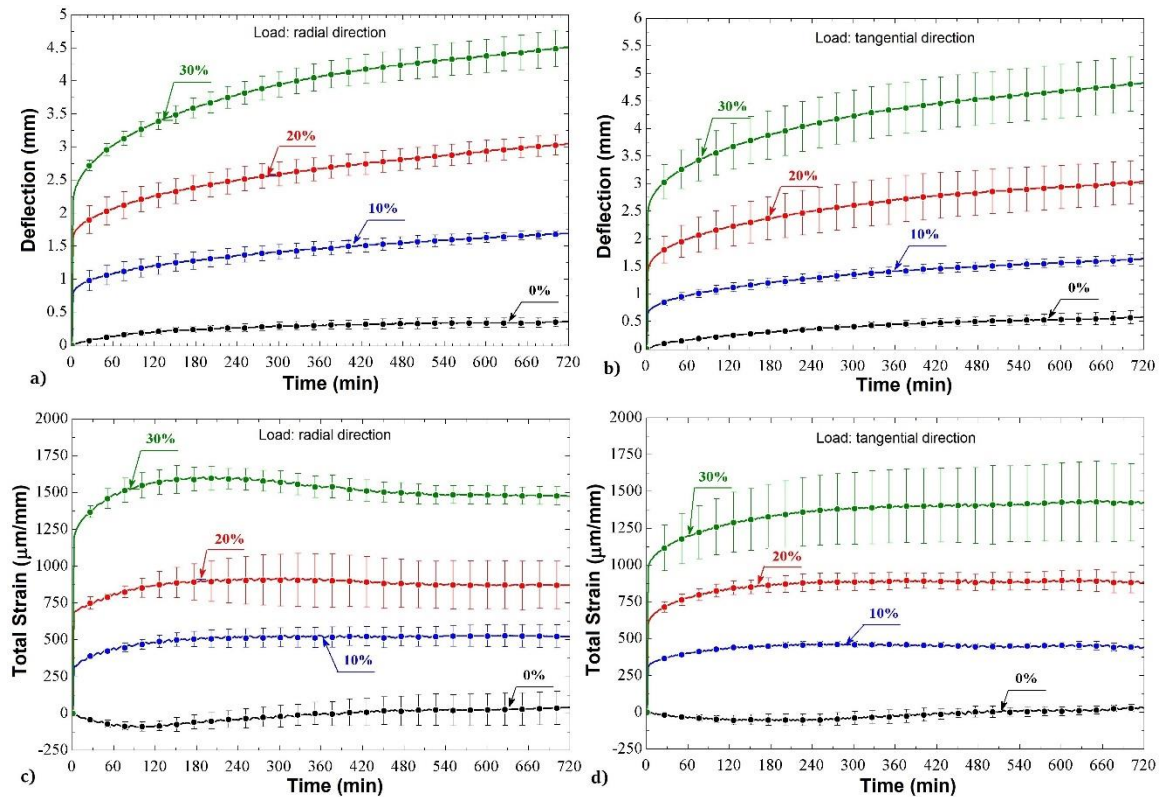


Fig. 8. Transient evolution of deflections and strains according to load application in radial and tangential directions. a): Transient evolution of deflection with load application in radial direction; and b): Transient evolution of deflection with load application in tangential direction; c): Total strain with load application in radial direction and d): Total strain with load application in tangential direction

Table 2 contains average values of instantaneous elastic strain, the free shrinkage strain, and the mechano-sorptive strain. As a result, the mechano-sorptive coefficient was calculated and presented. In this table, each one of the strain values was obtained for the loads applied in radial and tangential directions (see Fig. 3b and 3c). According to Table 2, for both directions of loading, the mechano-sorptive strain increased with the increment of the load. The magnitude order of mechano-sorptive strain was similar to the values verified from the literature (Muszynski *et al.* 2006). In particular, a higher total strain was observed when the load was applied in the radial direction; however, the average value of mechano-sorptive strain was lower for the same direction. The behavior for each strain component can be explained from the anatomical characteristics of the wood, and according to wood direction exposed to the load. According to Salvo *et al.* (2017), when the load is oriented in the tangential direction, the surface of the wood has a greater proportion of earlywood exposed to the load (Fig. 1). This wood characteristic tended to present lower values of microdensity, which resulted in a lower total strain when a load is

applied. This result for a load applied to the tangential direction was also reported by Gril (1988). On the other hand, the same anatomical characteristics influenced the results for the component strain by the mechano-sorption process. In this case, for a load applied to tangential direction, the wood presented a surface with lower values of microdensity, which resulted in a greater amount of wood-water interaction under the desorption process. This behavior led to higher mechano-sorptive strain when the load was applied in the tangential direction. According to the same table, the mechano-sorptive strain increased with the increment of the applied load in both directions. This result was due to the increase of the stress that increased proportionally with increasing load.

The last column of Table 2 corresponds to the average mechano-sorptive coefficient for the radial and tangential directions. These results are values calculated by the slope from the adjusted trend line on the strain-stress points illustrated in Fig. 9. According to this figure, the mean square errors of the trend lines presented values greater than $R^2 = 0.93$. The mechano-sorptive coefficient value obtained was 0.1746 (1/GPa) when the load applied was oriented in the tangential direction, and 0.1224 (1/GPa) for the load applied in the radial direction. These results corresponded to deformations measured with strain gages located at the longitudinal direction of a cantilever beam (see Fig. 3). In this aspect and for the same wood species, Pérez *et al.* (2016) have determined values of mechano-sorptive coefficients from deformations measured with strain gages located at radial and tangential directions. According to these authors, the values of mechano-sorptive coefficient are $msr = 1.71$ (1/GPa) and $ms_T = 5.30$ (1/GPa) for radial and tangential directions, respectively. These values are ten times higher than the coefficients calculated in this work with strain gages positioned in the longitudinal direction. Thus, according to the strain measurement direction, the mechano-sorptive coefficient can be organized and would present the following behavior in decreasing order: tangential/radial/longitudinal. This behavior was similar to the free shrinkage concerning the direction studied. According to Ananías *et al.* (2009), the free shrinkage of *Eucalyptus nitens* presents the following decreasing order: tangential/radial/longitudinal. Based on this behavior, and considering only the radial and tangential direction, the results obtained in this work are consistent with the values from the literature, and as shown in Table 2 and Fig. 9, the mechano-sorptive coefficient is higher when the tangential direction wood is positioned in the same direction as the action line of the applied load.

Table 2. Average Results on Strains and Mechano Sorptive Coefficient

| Load | | Strain ($\mu\text{m}/\text{m}$) | | | | | Mechano-Sorptive Coefficient (1/GPa) |
|------------|--------------|-----------------------------------|---------------------------------|----------------------|--------------------------------------|------------------------------|--------------------------------------|
| Direction | Breaking (%) | Elastic (ϵ_e) | Free Shrinkage (ϵ_M) | Total (ϵ) | Mechano Sorptive (ϵ_{ms}) | $\epsilon_e + \epsilon_{ms}$ | |
| Radial | 10 | 0.306 | 0.118 | 0.479 | 0.055 | 0.361 | 0.1224 |
| | 20 | 0.630 | | 0.862 | 0.114 | 0.744 | |
| | 30 | 0.903 | | 1.229 | 0.208 | 1.111 | |
| Tangential | 10 | 0.302 | 0.056 | 0.459 | 0.101 | 0.403 | 0.1746 |
| | 20 | 0.598 | | 0.876 | 0.222 | 0.820 | |
| | 30 | 0.887 | | 1.182 | 0.239 | 1.126 | |

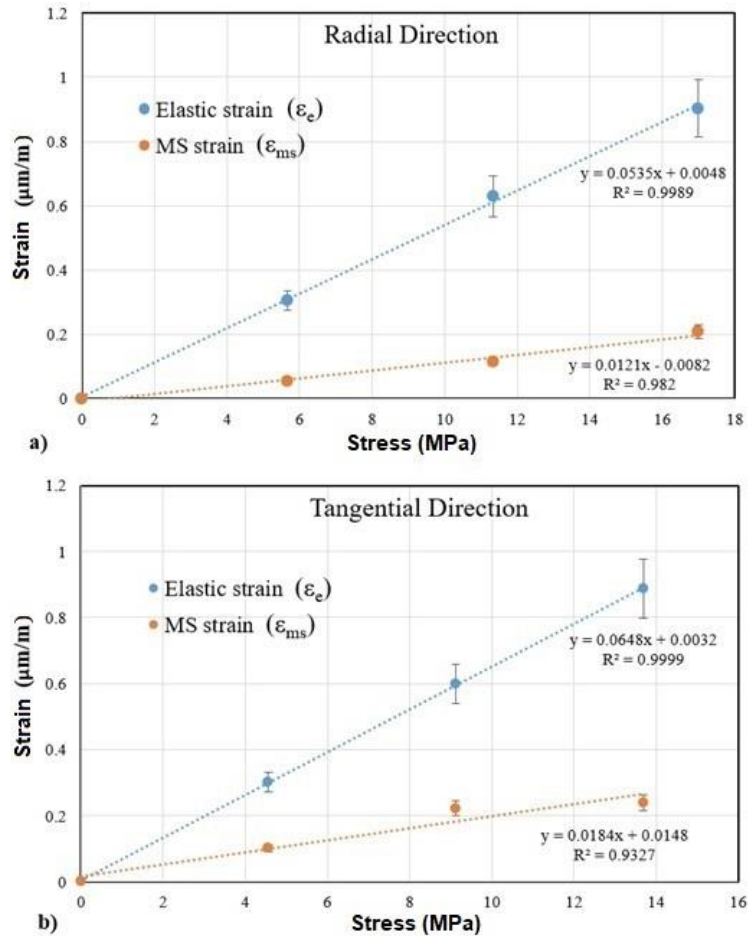


Fig. 9. Elastic and mechano-sorptive strains

CONCLUSIONS

1. The cantilever flexion tests subjected to moisture content (MC) variations below the fiber saturation point (FSP) were studied. The deformation effects caused by mechano-sorption process on the longitudinal direction were found. An average value of the mechano-sorptive coefficient in the longitudinal direction equal to 0.1485 GPa^{-1} was determined, which resulted in the order of ten times less than its similar value in the radial and tangential direction.
2. Samples loaded in the tangential direction experienced higher deformation values of mechano-sorptive strain. The ratio between the mechano-sorptive coefficient with radial *versus* the tangential load was 0.7010. Furthermore, a direct proportionality between the load intensity and the mechano-sorptive strain was observed for both sample positions.
3. The wood beams loaded in the radial direction were found to have the highest average modulus of elasticity (MOE) *versus* their equivalent value in the tangential direction.
4. The study conducted provided knowledge about the behavior of *Eucalyptus nitens* undergoing the mechano-sorption process.

ACKNOWLEDGEMENTS

The authors acknowledge Agencia Nacional de Investigación y Desarrollo, ANID-Chile for support received in the Fondo Nacional de Desarrollo Científico y Tecnológico, FONDECYT, project N°1160812.

Conflict of Interest

On behalf of all authors, the corresponding author states that there is no conflict of interest.

REFERENCES CITED

- Ananías, R. A., Sepúlveda, V., Pérez, N., Leandro, L., Salvo, L., Salinas, C., Cloutier, A., and Elustondo, D. (2014). "Collapse of *Eucalyptus nitens* wood after drying depending on the radial location within the stem," *Drying Technology* 32(14), 1699-1705. DOI: 10.1080/07373937.2014.924132
- Ananías, R. A., Díaz, C., and Leandro, L. (2009). "Estudio preliminar de la contracción y el colapso en *Eucalyptus nitens* [Preliminary study of shrinkage and collapse in *Eucalyptus nitens*]," *Maderas-Ciencia y Tecnología* 11(3), 251-260. DOI: 10.4067/S0718-221X2009000300007
- Armstrong, L. D., and Christensen, G. N. (1961). "Influence of moisture content on deformation of wood under stress," *Nature* 191, 869-870.
- Chávez, C., Moraga, N., Salinas, C., Cabrales, R., and Ananías, R. A. (2021). "Modeling unsteady heat and mass transfer with prediction of mechanical stresses in wood drying," *International Communications in Heat and Mass Transfer* 123(2), DOI: 10.1016/j.icheatmasstransfer.2021.105230
- Derikvand, M., Nolan, J., Jiao, H., and Koltarewsky, N. (2017). "What to do with structurally low-grade wood from Australian's plantation eucalypts, building application," *BioResources* 12(1),4-7. DOI: 10.15376/biores.12.1.4-7
- Florisson, S., Ormansson, S., and Vessby, J. (2019). "A numerical study of green-state moisture content on stress development in timber boards during drying," *Wood and Fiber Science* 51(1), 41-57. DOI: 10.22382/wfs-2019-005
- Gril, J. (1988). *Une Modélisation du Comportement Hygro-rhéologique du Bois à Partir de sa Microstructure [A modeling of the hygro-rheological behavior of wood from its microstructure]*, PhD thesis, University of Paris, France.
- Grossman, P. U. A. (1976). "Requirements for a model that exhibits mechano-sorptive behavior," *Wood Science and Technology* 10, 163-168.
- Hsieh, T. Y., and Chang, F. C. (2018). "Effects of moisture content and temperature on wood creep," *Holzforschung* 72(12), 1071-1078. DOI: 10.1515/hf-2018-0056
- Huang, Y. (2016). "Creep behavior of wood under cyclic moisture changes: Interaction between load effect and moisture effect," *Journal of Wood Science* 62(5), 392-399. DOI: 10.1007/s10086-016-1565-4
- Hering, S., and Niemz, P. (2012). "Moisture-dependent, viscoelastic creep of European beech wood in longitudinal direction," *European Journal of Wood and Wood Products* 70(5), 667-670. DOI: 10.1007/s00107-012-0600-4

- Huc, S., Svensson, S., and Hoznan, T. (2018). "Higro-mechanical analysis of wood subjected to constant mechanical load and varying relative humidity," *Holzforschung* 72(10), 863-870. DOI: 10.1515/hf-2018-0035
- INFOR. (2018). "La industria del aserrío. Boletín Estadístico N° 165 [*The sawmill industry. Statistical Bulletin N° 165*]," Instituto Forestal, Santiago, Chile. 158p.
- Kaboorani, A., Blanchet, P., and Laghdar, A. (2013). "A rapid method to assess viscoelastic and mechano-sorptive creep in wood," *Wood and Fiber Science* 45(4), 370-382.
- Martensson, A. (1994). "Mechano-sorptive effects in wooden material," *Wood Science and Technology* 28(6), 437-449. DOI: 10.1007/BF00225463
- McKimm, R. (1985). "Characteristics of the wood of young fast-grown trees of *Eucalyptus nitens* maiden with special reference to provenance variation. II. Strength, dimensional stability and preservation characteristics," *Australian Forest Research* 15(2), 219-234.
- Muszynski, L., Lagana, R., and Shaler, S. (2006). "Hygro-mechanical behavior of red spruce in tension parallel to the grain," *Wood and Fiber Science* 38(1), 155-165.
- Navi, P., and Heger, F. (eds.) (2005). *Comportement Thermo-hydrromécanique du Bois [Thermo-hydrromechanical behavior of wood]*, Presses Polytechniques et Universitaires Romandes, Lausanne, Switzerland
- Ormarsson, S., Cown, D., and Dahlblom, O. (2003). "Finite element simulations de moisture related distortion in laminated timber products of Norway spruce and radiata pine," *8th IUFRO International Wood Drying Conference*, pp. 27-33.
- Pang, S. (2000). "Modelling of stress development during drying and relief during steaming in *Pinus radiata* lumber," *Drying Technology* 18(8), 1677-1696. DOI: 10.1080/07373930008917806
- Peng, H., Lu, J., Jiang, J., and Cao, J. (2017). "Longitudinal mechano-sorptive creep behavior of Chinese fir in tension during moisture adsorption processes," *Materials* 10(8), 931. DOI: 10.3390/ma10080931
- Pérez, N., Chávez, C., Salinas, C., and Ananías, R. A. (2018). "Simulation of drying stresses in *Eucalyptus nitens* wood," *BioResources* 13(1), 1413-1424. DOI: 10.15376/biores.13.1.1413-1424
- Pérez, N., Cloutier, A., Segovia, F., Salinas, C., Sepúlveda, V., Salvo, L., Elustondo, D. M., and Ananias, R. A. (2016). "Hygromechanical strains during the drying of *Eucalyptus nitens* boards," *Maderas-Ciencia y Tecnología* 18(2), 235-244. DOI: 10.4067/S0718-221X2016005000021
- Ranta-Maunus, A. (1993). "Rheological behavior of wood in directions perpendicular to the grain," *Materials and Structures* 26(6), 362-369. DOI: 10.1007/BF02472962
- Ranta-Maunus, A. (1975). "The viscoelasticity of wood at varying moisture content," *Wood Science and Technology* 19, 189-205. DOI: 10.1007/BF00364637
- Rebolledo, P., Salvo, L., Contreras, H., Cloutier, A., and Ananias, R. A. (2013). "Variation of internal checks related with anatomical structure and density in *Eucalyptus nitens* wood," *Wood and Fiber Science* 45(3), 279-286.
- Salinas, C., Chávez, C., Ananías, R.A., and Elustondo, D. (2015). "Unidimensional simulation of drying stress in Radiata pine wood," *Drying Technology* 33(8), 996-1005. DOI: 10.1080/07373937.2015.1012767

- Salvo, L., Leandro, L., Contreras, H., Cloutier, A., Elustondo, D., and Ananias, R.A. (2017). "Radial variation of density and anatomical features in *Eucalyptus nitens* trees," *Wood and Fiber Science* 49(3), 301-311.
- Sepúlveda, V., Pérez, N., Salinas, C., Salvo, L., Elustondo, D., and Ananías, R.A. (2016). "The development of moisture and strain profiles during pre-drying of *Eucalyptus nitens*," *Drying Technology* 34(4), 428-436. DOI: 10.1080/07373937.2015.1060490

Article submitted: October 17, 2021; November 21, 2021; Revised version received and accepted: December 10, 2021; Published: December 16, 2021.
DOI: 10.15376/biores.17.1.1047-1061

NOMENCLATURE

| | | |
|---------------|------------------------------|-------------------|
| EMC | Equilibrium moisture content | [%] |
| FSP | Fiber saturation point | [%] |
| I | Moment of inertia | [m ⁴] |
| MC | Moisture content | [%] |
| P | Load | [N] |
| T | Temperature | [°C] |
| ms | Mechano-sorptive coefficient | [1/GPa] |
| Greek symbols | | |
| σ | Stress | [Pa] |
| ε | Strain | [dimensionless] |
| δ | Displacement/deflection | [m] |
| Subscripts | | |
| p | Plastic | |
| e | Elasticity | |
| ms | Mechano-sorptive | |
| v | Viscoelasticity | |
| db | Dry bulb | |
| w | Wet | |
| wb | Wet bulb | |
| 0 | Dry conditions | |
| M | Free strain | |
| R | Radial | |
| T | Tangential | |